Circular Dichroism of Chromium(III) Complexes. V. Circular Dichroism of *trans*-Dihalogenobis(diamine) Complexes with Optically Active Diamines

Sumio Kaizaki and Yoichi Shimura

Department of Chemistry, Faculty of Science, Osaka University, Toyonaka, Osaka 560

(Received June 19, 1975)

Nine chromium(III) complexes of *trans*-$[CrX_2(N)_4]$ type with three kinds of optically active diamines (*R*-propylenediamine, *S*,*S*-stilbenediamine and *S*,*S*-2,4-pentanediamine) were prepared and the absorption and circular dichroism spectra were measured in the region of their d–d transitions. The CD behaviors in the spin-allowed transitions were discussed in comparison with the corresponding cobalt(III) complexes and their bands were assigned to the tetragonal components. On the basis of the theoretical correlation between the rotational strengths for the spin-forbidden transitions and for the spin-allowed transitions, the CD peaks in the spin-forbidden transitions were discussed and assigned.

In the previous paper,[1)] circular dichroism (CD) spectra of optically active tris-chelate chromium(III) complexes in the spin-forbidden transitions have been reported and analyzed in connection with the CD in the spin-allowed transitions in terms of the theoretical correlation between the rotational strengths in the spin-forbidden and the spin-allowed transitions. Since there have remained some ambiguities about the assignment of the trigonal splitting CD components in the spin-allowed transitions, alternative assignments may be possible. On the other hand, it has been well known that for so-called praseo type complexes the first spin-allowed bands of octahedral parantage split largely enough to resolve the tetragonal components in solution absorption spectra at room temperature and this allows to make the band assignment feasible. On the basis of analyses of absorption spectra as well as crystal field approximation treatments,[2–7)] the assignments of spin-allowed d–d transitions of chromium(III) complexes in tetragonal field have been made rigorously, and the tetragonal crystal field parameters, *Dt* and *Ds*, and/or the angular overlap model (AOM) parameters, $\delta\sigma$ and $\delta\pi$,[8)] have been derived and discussed.[2–7,9)] By using these parameters, the positions and the splittings of the doublet states can also be estimated.[10)] Thus, the observation of the spin-forbidden bands provides a criterion for testing the crystal field or AOM parameters. Some absorption and emission data in the spin-forbidden transitions have been reported[11–15)] and their peaks have been assigned according to the crystal field theory. The CD in the spin-forbidden transitions will be expected to offer more detailed information, because the rotational strengths for these transitions are theoretically related to those for the spin-allowed transitions. Nevertheless, there has been no report on the CD spectra of tetragonal complexes with optically active diamines not only in the spin-allowed transitions but also in the spin-forbidden transitions, though optical activity of the corresponding Co(III) complexes has been intensively studied in the spin-allowed transitions.[16–19)]

In this paper, nine *trans*-$[CrX_2(N)_4]$ type complexes with three kinds of optically active diamines (*R*-propylenediamine=*R*-pn, *S*,*S*-stilbenediamine=*S*,*S*-stien and *S*,*S*-2,4-pentanediamine=*S*,*S*-2,4-ptn) have been prepared and their absorption and CD spectra have been measured in their spin-allowed and spin-forbidden transition regions. The theoretical correlation between the rotational strengths for the spin-forbidden and spin-allowed transitions will be presented in a manner similar to the trigonal complexes, but in a more refined form including the configuration interaction and molecular orbital extension to the spin-orbit coupling effect on axial ligands.

Experimental

Preparation of Optically Active Diamines. *1)* R-*Propylenediamine*: This was resolved through its tartrate and isolated as free diamine.

2) S,S-*Stilbenediamine*: The racemic diamine was prepared by the method of Williams and Bailar,[20)] and resolved into the enantiomer through its tartrate by the method of Lifschitz and Bos.[21)]

3) R,R- *or* S,S-*2,4-Pentanediamine*: This was prepared and resolved by the method of Bosnich,[19)] and isolated as its dihydrogen dichloride.

Preparation of the Complexes. The fluoro complexes were prepared by the method analogous to Glerup *et al.*'s.[22)] The conversion of the fluoro complexes to the chloro and bromo complexes was carried out by the modified method of Fee *et al.*[23)]

The R-*Propylenediamine Complexes.* *1)* trans-$[CrF_2(R\text{-}pn)_2]ClO_4\cdot H_2O$: This complex was obtained by the method of Glerup *et al.*[22)] Found: C, 19.97; H, 6.35; N, 15.39%. Calcd for *trans*-$[CrF_2(R\text{-}pn)_2]ClO_4\cdot H_2O$: C, 20.26; H,6.23; N, 15.75%.

2) trans-$[CrCl_2(R\text{-}pn)_2]ClO_4$: *trans*-$[CrF_2(R\text{-}pn)_2]ClO_4\cdot H_2O$ (12 g) was dissolved in 15 cm^3 of 40—44% hydrochloric acid, which was obtained by bubbling hydrogen chloride to concentrated hydrochloric acid at 0 °C. The dark red solution obtained was kept with stirring for a while at room temperature; then red crystals were precipitated. The color of the separated crystals was grayish green with a reddish tint. The yield was about 8 g. Recrystallization was carried out from methanol–ether. Found: C, 18.91; H, 5.66; N, 15.10%. Calcd for *trans*-$[CrCl_2(R\text{-}pn)_2]ClO_4$: C, 19.45; H, 5.44; N, 15.12%.

3) trans-$[CrBr_2(R\text{-}pn)_2]Br\cdot H_2O$: One gram of *trans*-$[CrF_2(R\text{-}pn)_2]ClO_4\cdot H_2O$ was dissolved in 3 cm^3 of 48% hydrobromic acid, and the mixture was stirred for a while at room temperature. The complex was obtained as a green precipitate; the yield was about 0.3 g. This was recrystallized from methanol–ether. This complex was also obtained in good yield from the reaction in 3.5 M methanolic hydrogen bromide solution. Found: C, 15.70; H, 4.83; N, 11.98%. Calcd for *trans*-$[CrBr_2(R\text{-}pn)_2]Br\cdot H_2O$: C, 15.74; H, 4.84; N, 12.23%.

The S,S-*Stilbenediamine Complexes.* *1)* trans-[*Cr*F_2(S,S-*stien*)$_2$]*Cl*O_4·H_2O: *trans*-[$CrF_2(py)_4$]ClO_4[22] (17.5 g) was dissolved in 100 cm^3 of hot 2-methoxyethanol. To the resulting violet solution was added 14 g *S,S*-stilbenediamine, and then the solution was refluxed for a while. The red solution obtained was condensed by a vacuum rotary evaporator. The red orange precipitate was obtained by adding the condensed solution to water. This was dissolved in methanol, filtered and the pinkish orange crystals were precipitated by adding ether. The color of the filtrate was red. The pinkish orange compound was insoluble in acetone, while the red one was soluble in acetone. The purification of this pinkish orange complex was performed by adding the methanolic solution to acetone. Found: C, 53.49; H, 5.49; N, 8.90%. Calcd for *trans*-[CrF_2(*S,S*-stien)$_2$]ClO_4·H_2O: C, 53.20; H, 5.42; N, 8.86%.

2) trans-[*Cr*Cl_2(S,S-*stien*)$_2$]*Cl*·2H_2O: To 47% methanolic hydrogen chloride solution was added 0.55 g of *trans*-[CrF_2(*S,S*-stien)$_2$]ClO_4·H_2O. The color of the solution changed to dark red. Then the reaction mixture was poured into water. The pale green powder was obtained. This was recrystallized from methanol-ether. Found: C, 54.27; H, 5.87; N, 9.03%. Calcd for *trans*-[$CrCl_2$(*S,S*-stien)$_2$]Cl·2H_2O: C, 54.33; H, 5.86; N, 9.05%.

3) trans-[*Cr*Br_2(S,S-*stien*)$_2$]*Br*·CH_3OH: *trans*-[CrF_2(*S,S*-stien)$_2$]ClO_4·H_2O (1 g) was suspended in 20 cm^3 of 3.5 M methanolic hydrogen bromide solution. The starting complex was gradually dissolved during about one hour. After stirring for about two hours, the color of the solution turned to green. The resulting solution was poured into water. Then the desired complex was obtained as a green precipitate. This was recrystallized from methanol-ether. Found: C, 46.34; H, 4.83; N, 7.62%. Calcd for *trans*-[$CrBr_2$(*S,S*-stien)$_2$]Br·CH_3OH: C, 46.55; H, 4.85; N, 7.49%.

The S,S-*2,4-pentanediamine complexes.* *1)* trans-[*Cr*F_2(S,S-*2,4-ptn*)$_2$]*Cl*O_4: Pure sodium (1.1 g) was dissolved in 30 cm^3 of 2-methoxyethanol. To this solution was added 4 g of *S,S*-2,4-ptn·2HCl by portions; then white powder of sodium chloride was precipitated. During this procedure, dry nitrogen gas was bubbled into the solution in order to protect from carbon dioxide and moisture. The sodium chloride was removed by filtration, and washed with a small amount of 2-methoxyethanol. To the combined filtrate and washings was added 5 g of *trans*-[$CrF_2(py)_4$]ClO_4. The mixture was heated on a steam bath and then orange crystals were precipitated. This product was contaminated by a small amount of impurities such as chromium(III) hydroxide. The recrystallization was carried out from the aqueous solution which was slightly acidified with a small amount of $HClO_4$. The yield was about 2.3 g. Found: C, 30.42; H, 7.24; N, 14.20%. Calcd for *trans*-[CrF_2(*S,S*-2,4-ptn)$_2$]ClO_4: C, 30.50; H, 7.17; N, 14.23%.

2) trans-[*Cr*Cl_2(S,S-*2,4-ptn*)$_2$]*Cl*O_4: In a 5 cm^3 portion of concentrated hydrochloric acid was dissolved 0.7 g of *trans*-[CrF_2(*S,S*-2,4-ptn)$_2$]ClO_4, and the mixture was allowed to stand for 3—4 hr. Green needles were precipitated. They were recrystallized from methanol-ether. Found: C, 28.19; H, 6.67; N, 13.34%. Calcd for *trans*-[$CrCl_2$(*S,S*-2,4-ptn)$_2$]ClO_4: C, 28.21; H, 6.63; N, 13.16%.

3) trans-[*Cr*Br_2(S,S-*2,4-ptn*)$_2$]*Br*: *trans*-[CrF_2(*S,S*-2,4-ptn)$_2$]ClO_4 (1 g) was dissolved in a small amount of 4 M ethanolic hydrogen bromide. The solution was allowed to stand over night in a refrigerator. Then light green leaflets were obtained. They were recrystallized from methanol-ether. Found: C, 24.03; H, 5.77; N, 11.30%. Calcd for *trans*-[$CrBr_2$(*S,S*-2,4-ptn)$_2$]Br: C, 24.21; H, 5.68; N, 11.29%.

Measurements. The electronic absorption spectra were measured by a Shimadzu spectrophotometer UV-200. The CD spectra were recorded with a Jasco MOE-1 spectropolarimeter. The CD measurements were carried out with the wavelength expansion of 4 nm/cm and 10 nm/cm in the spin-forbidden and spin-allowed transition regions, respectively. Therefore, four significant figures were used in expressing wave numbers in the spin-forbidden transition region, whereas three significant figures were used in the spin-allowed transition region. The concentrations of the complexes for the CD measurements in the spin-forbidden transition region were 10^{-1} to 10^{-2} mol dm^{-3}, and the cell lengths employed were 5 and 10 cm. The absorption and CD spectra of the fluoro complexes with *R*-pn and *S,S*-ptn were measured in water, while those of the other complexes in methanol.

Results and Discussion

1) Absorption Spectra. The ligand field absorption spectra of the nine complexes concerned are given in Figs. 1—3, and their characteristics are listed in Table 1. It is noted that their absorption patterns are similar, on the whole, to those of the corresponding *trans*-dihalogenobis(ethylenediamine)chromium(III) complexes, being independent of the optically active diamines and only dependent on the axial ligands. That is, for the fluoro complexes, two split components are observed in both the first $^4T_2 \leftarrow {}^4A_2$ and the second $^4T_1 \leftarrow {}^4A_2$ spin-allowed octahedral transition regions, whereas the other complexes show two largely split components in the first band region and only one in the second band region as in Figs. 1—3. The higher frequency component in the first band region shifts scarcely for any halogeno complexes and lies at about 22000 cm^{-1}, where the first absorption band of [$Cr(N)_6$] type complex is expected. While the lower frequency component shifts to the lower frequency side in the order of fluoro, chloro and bromo complexes. This order is in coincidence with spectrochemical series of the axial halogeno ligands.[21]

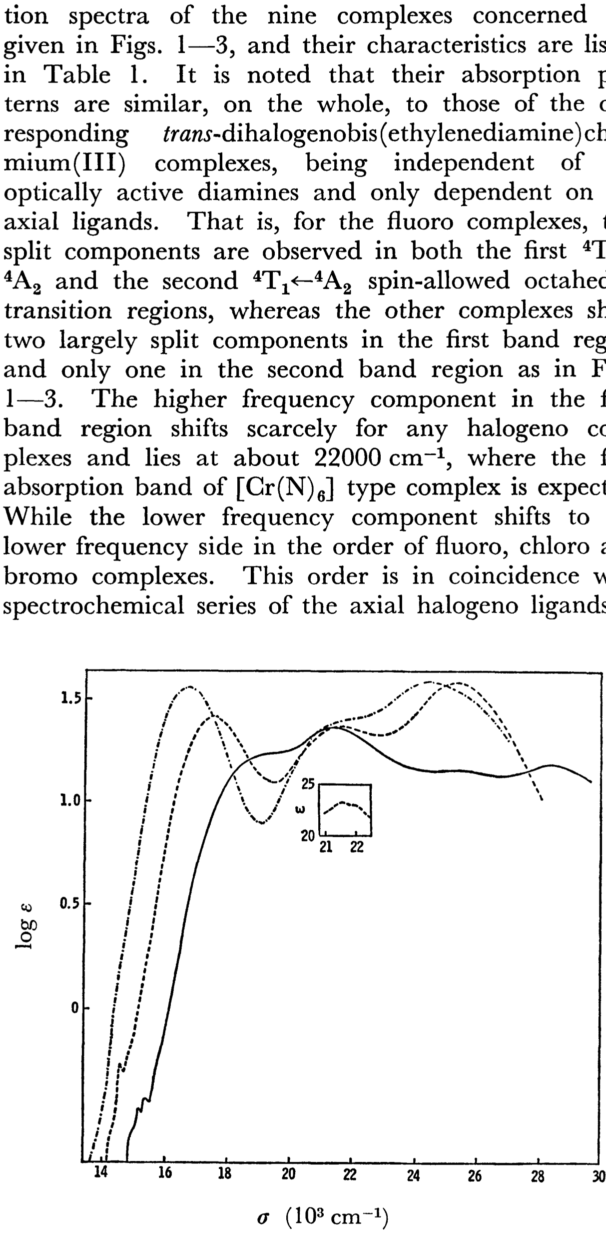

Fig. 1. Absorption curves of *trans*-[CrX_2(*R*-pn)$_2$]$^+$, X=F (——) in water; X=Cl (----) in methanol; X=Br (—·—·—) in methanol.

TABLE 1. ABSORPTION (AB) AND CD DATA FOR TETRAGONAL CHROMIUM(III) COMPLEXES IN THE d–d TRANSITIONS (Wave numbers are in 10^3 cm^{-1}; CD intensities asterisked are multiplied by 10^3)

AB (log ε_{max})		CD ($\Delta\varepsilon_{ext}$)		Assignment
trans-[CrF_2(*R*-pn)$_2$]$ClO_4\cdot H_2O$				
		13.33	(+0.67*)	$^2E(^2T_1)$
		14.50	(+0.93*)	
14.92$^{a)}$		14.73	(+1.35*)	$^2B_1(^2E)$
15.08	($\bar{1}$.52)	15.03	(+9.96*)	$^2A_1(^2E)$
15.33	($\bar{1}$.56)	15.30$^{a)}$	(+2.4*)	$^2A_2(^2T_1)$
		15.55	(+4.49*)	
		15.68	(−0.56*)	
		15.79	(+5.08*)	
19.3$^{a)}$	(1.24)	18.8	(+0.41)	$^4E(^4T_2)$
21.5	(1.36)	22.0	(−0.15)	$^4B_2(^4T_2)$
25.0	(1.16)			$^4E(^4T_1)$
28.5	(1.18)	29.7	(−0.0043)	$^4A_2(^4T_1)$
trans-[$CrCl_2$(*R*-pn)$_2$]ClO_4				
		14.08	(+0.71*)	
		14.33	(+2.78*)	$^2A_1(^2E)$
14.52	($\bar{1}$.73)	14.58	(+0.45*)	$^2B_1(^2E)$
		14.70	(−0.13*)	$^2E(^2T_1)$
		14.90$^{a)}$	(+0.30*)	
		15.02	(+1.11*)	$^2A_2(^2T_1)$
		15.19	(−0.73*)	
		15.36	(−0.21*)	
17.5	(1.43)	17.7	(+0.37)	$^4E(^4T_2)$
21.7	(1.39)	21.7	(−0.09)	$^4B_2(^4T_2)$
25.3	(1.60)	25.7	(+0.11)	$^4E(^4T_1)$
trans-[$CrBr_2$(*R*-pn)$_2$]Br				
		14.08	(−1.26*)	$^2E(^2T_1)$
		14.29	(+0.28*)	$^2A_1(^2E)$
		14.39	(−0.98*)	$^2B_1(^2E)$
		14.55	(−0.49*)	
		14.65	(+0.53*)	$^2A_2(^2T_1)$
		14.88	(−0.50*)	
16.7	(1.57)	17.0	(+0.35)	$^4E(^4T_2)$
22.0	(1.40)	21.3	(−0.06)	$^4B_2(^4T_2)$
24.6	(1.58)	26.0	(+0.13)	$^4E(^4T_1)$
trans-[CrF_2(*S*,*S*-stien)$_2$]$ClO_4\cdot H_2O$				
		12.71	(−0.50*)	$^2E(^2T_1)$
		13.58	(−1.14*)	
14.12	(0.00)	13.92	(−1.81*)	
15.00	(0.005)	14.65	(−6.54*)	$^2B_1(^2E)$
15.29	(0.037)	14.95	(−22.9*)	$^2A_1(^2E)$
		15.21	(−5.20*)	$^2A_2(^2T_1)$
		15.44	(−8.60*)	
19.0$^{a)}$		18.9	(−0.80)	$^4E(^4T_2)$
21.2	(1.61)	20.7$^{a)}$	(−0.52)	$^4B_2(^4T_2)$
25.0$^{a)}$		25.0	(+0.13)	$^4E(^4T_1)$
29.5	(1.36)			$^4A_2(^4T_1)$
trans-[$CrCl_2$(*S*,*S*-stien)$_2$]$Cl\cdot H_2O$				
		14.27	(−9.95*)	$^2A_1(^2E)$
14.50	(0.16)	14.50	(−3.32*)	$^2B_1(^2E)$
		14.81	(−0.97*)	$^2E(^2T_1)$
		15.07	(−2.75*)	$^2A_2(^2T_1)$
		15.33	(−3.44*)	
17.7	(1.50)	17.6	(−0.60)	$^4E(^4T_2)$
22.1	(1.62)	21.7	(−0.58)	$^4B_2(^4T_2)$
		22.0	(−0.60)	
25.5	(1.80)	25.7	(−0.35)	$^4E(^4T_1)$
trans-[$CrBr_2$(*S*,*S*-stien)$_2$]$Br\cdot CH_3OH$				
		14.26	(−5.58*)	$^2A_1(^2E)$
		14.43	(−2.65*)	$^2B_1(^2E)$
		14.57	(−3.50*)	$^2A_2(^2T_1)$
16.9	(1.74)	17.0	(−0.52)	$^4E(^4T_2)$
22.0	(1.67)	21.5$^{a)}$	(−0,59)	$^4B_2(^4T_2)$
		21.8	(−0.60)	
24.5	(1.77)	24.0$^{a)}$	(−0.40)	$^4E(^4T_1)$
trans-[CrF_2(*S*,*S*-2,4-ptn)$_2$]ClO_4				
		13.95	(−0.99*)	$^2E(^2T_1)$
14.95	($\bar{1}$.84)	14.85	(+6.30*)	$^2B_1(^2E)$
15.11	($\bar{1}$.94)	15.08	(−4.92*)	$^2A_1(^2E)$
15.33	($\bar{1}$.96)	15.50	(+6.10*)	
		15.73	(+16.5*)	
		16.42	(+23.8*)	
18.5	(1.28)	18.7	(−0.31)	$^4E(^4T_2)$
21.3	(1.36)	21.7	(+0.53)	$^4B_2(^4T_2)$
25.0	(1.26)			$^4E(^4T_1)$
27.8	(1.26)	28.3	(+0.016)	$^4A_2(^4T_1)$
trans-[$CrCl_2$(*S*,*S*-2,4-ptn)$_2$]ClO_4				
		13.75$^{a)}$	(+0.5*)	
		14.00$^{a)}$	(+2.0*)	
		14.26	(+3.74*)	
14.45		14.41	(−1.65*)	$^2A_1(^2E)$
		14.59	(+7.10*)	$^2B_1(^2E)$
		14.88$^{a)}$	(+8.85*)	$^2E(^2T_1)$
		15.07	(+15.0*)	
		15.31	(+18.9*)	
		15·53	(+18.4*)	
17.0	(1.44)	17.3	(−0.31)	$^4E(^4T_2)$
21.3	(1.37)	21.2	(+0.33)	$^4B_2(^4T_2)$
		22.2$^{a)}$		
25.0	(1.66)	25.7	(−0.32)	$^4E(^4T_1)$
trans-[$CrBr_2$(*S*,*S*-2,4-ptn)$_2$]Br				
		14.33	(+14.8*)	
		14.51	(+19.8*)	
		14.64	(+25.7*)	
		14.77$^{a)}$	(+22.6*)	
		15.00$^{a)}$	(+20.0*)	
16.3	(1.53)	16.7	(−0.20)	$^4E(^4T_2)$
21.0$^{a)}$	(1.33)	21.1	(+0.20)	$^4B_2(^4T_2)$
		21.8	(+0.19)	
24.7	(1.55)	25.7	(−0.47)	$^4E(^4T_1)$

---

a) shoulder.

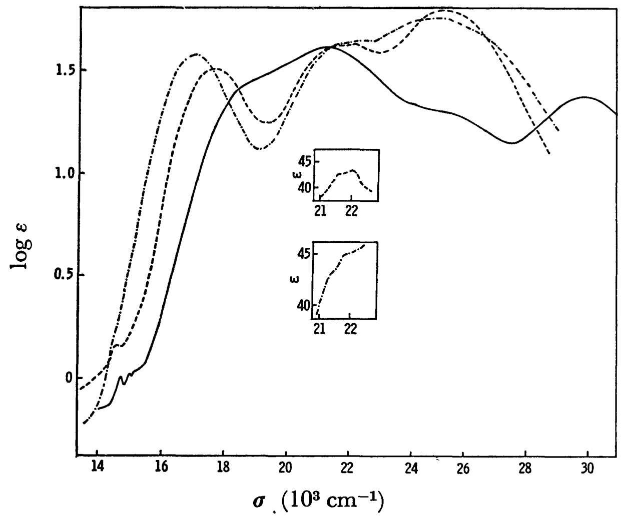

Fig. 2. Absorption curves of *trans*-[CrX_2(*S*,*S*-stien)$_2$]$^+$ X=F (——); X=Cl (----); X=Br (—·—·—) in methanol.

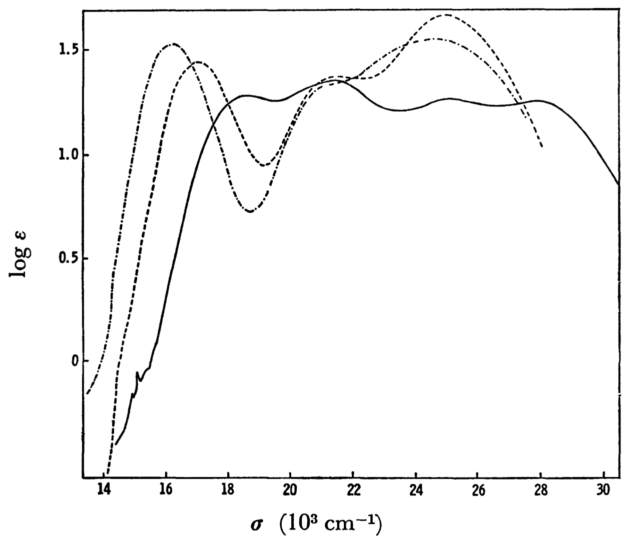

Fig. 3. Absorption curves of *trans*-[CrX_2(*S*,*S*-2,4-ptn)$_2$]$^+$, X=F (——) in water; X=Cl (----) in methanol; X=Br (—·—·—) in methanol.

Since these absorption behavior agrees with the expectation from the ligand field theory[2] and the angular overlap model[6] for tetragonal chromium(III) complexes, the higher frequency and the lower frequency components in the first band region are due to the $^4E \leftarrow$ and $^4B_2 \leftarrow {}^4B_1$ transition, respectively. This assignment has been unequivocally confirmed from single crystal polarized absorption spectra of *trans*-dihalogenobis(ethylenediamine)Cr(III) complexes.[4]

Both the split components, ^4E and $^4B_2$, in the first band region of the dichloro and dibromo complexes are found to shift to the lower frequency side in the order of *S*,*S*-stien, *R*-pn and *S*,*S*-2,4-ptn complexes. This fact suggests that the ligand field of the diamines decreases in this order as found in the case of the corresponding cobalt(III) complexes.[18,19]

The molar absorptivities of the $^4B_2$ components for the fluoro, chloro, and bromo complexes with a given diamine are close to each other, whereas those of the ^4E components increase in the order of the fluoro, chloro, and bromo complexes. This order is consistent with the hyperchromic series of the axial ligands.[25] The $^4B_2$ components of *trans*-[$CrCl$]$_2$(*R*-pn)$_2$]$^+$ and *trans*-[CrX_2(*S*,*S*-stien)$_2$]$^+$ (X=Cl, Br) split by some 500—800 cm^{-1}. This splitting may result from a strong spin-orbit coupling between the $^2\Gamma(^2T_2)$ and $^4B_2$ states as discussed later.

In the lower frequency region, where the doublet$\leftarrow$quartet spin-forbidden transitions occur, some weak but sharp peaks or inflections are observed for the fluoro and chloro complexes, but none for the bromo complexes as shown in Figs. 1—3. The absorption intensities of spin-forbidden bands are found to be one twentieth to one fiftieth times as weak as those of the spin-allowed bands. The spin-forbidden transitions of the fluoro complexes are shifted to the lower frequency than those of the chloro complexes.

2) CD Spectra in the First Spin-allowed Transitions. Two CD components associated with the first $^4E \leftarrow$ and $^4B_2 \leftarrow {}^4B_1$ spin-allowed transitions are observed for all the complexes concerned in Figs. 4—6. The CD patterns depend largely on the optically active diamines and independent of the axial ligands. That is, for the *R*-pn complexes, a large positive and a small negative CD component is observed in the region corresponding to the lower frequency ^4E and the higher frequency $^4B_2$ absorption band, respectively. For

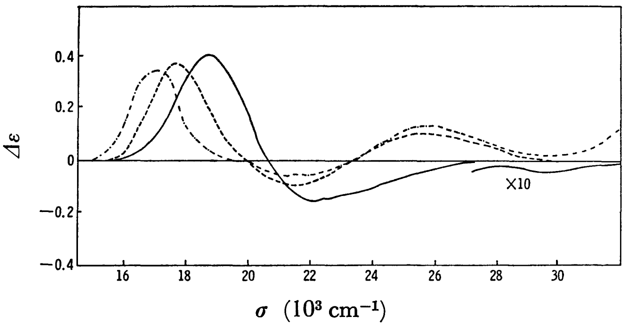

Fig. 4. CD curves in the spin-allowed transitions of *trans*-[CrX_2(*R*-pn)$_2$]$^+$, X=F (——) in water; X=Cl (----) in methanol; X=Br (—·—·—) in methanol.

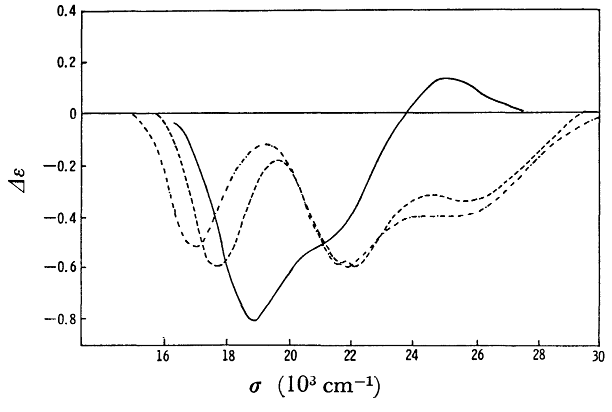

Fig. 5. CD curves in the spin-allowed transitions of *trans*-[CrX_2(*S*,*S*-stien)$_2$]$^+$, X=F (——); X=Cl (----); X=Br (—·—·—) in methanol.

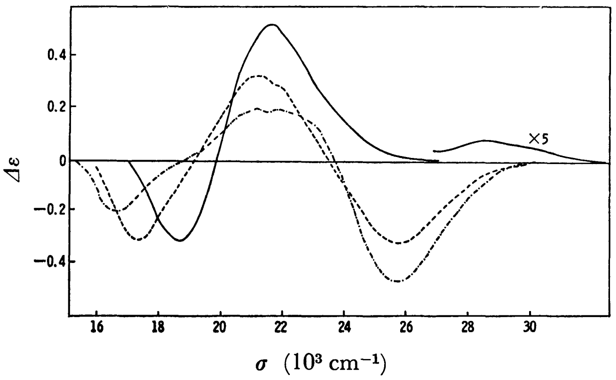

Fig. 6. CD curves in the spin-allowed transitions of *trans*-[CrX_2(*S*,*S*-2,4-ptn)$_2$]$^+$, X=F (——) in water; X=Cl (----) in methanol; X=Br (—·—·—) in methanol.

the *S*,*S*-stien complexes, two negative CD bands are observed in this region. The *S*,*S*-2,4-ptn complexes show two CD components with opposite signs, (−) and (+) from the longer wavelength side, having nearly equal area. Such CD behavior of chromium(III) complexes is quite similar to the corresponding cobalt(III) complexes.[18,19,26] Therefore, it seems reasonable that the coordinated optically active diamines in the chromium(III) complexes take the same conformations as those in the cobalt(III) complexes. That is, the conformation of the *R*-pn, *S*,*S*-stien and *S*,*S*-2,4-ptn is assigned to λ-,[27] δ-*gauche*[26b] and δ-twist[18] form, respectively.

The CD intensities of the chromium(III) complexes are found to be about half as compared with those of the corresponding cobalt(III) complexes, as predicted by a general theory on CD of metal complexes.[28]

3) CD Spectra in the Second Spin-allowed Transitions. One CD component associated with the second $^4T_1$←$^4A_2$ octahedral transition of the chloro or bromo complex is observed at the higher frequency side than the absorption band, as in Figs. 4—6 and Table 1, indicating that the CD band is ascribed to the $^4E_b(^4T_1)$ component which lies at the higher frequency than the $^4A_2(^4T_1)$ component as is predicted theoretically and confirmed by single crystal polarized absorption spectra.[4] These CD bands are of the same signs as those of the $^4E_a(^4T_2)$ components. The CD band of the fluoro complexes with *R*-pn and *S*,*S*-2,4-ptn observed in the second band region lies rather closely to the $^4A_2$ absorption component, and therefore this band is assigned to the $^4A_2$←$^4B_1$ transition which may be vibronically allowed by lowering symmetry through the mixing with the $^4B_2$ component, as has been observed for *trans*-[CoCl]$_2$(*R*-pn)$_2$]$^+$.[30] The CD intensities of these bands are found to be much weaker than those of the $^4E_b(^4T_1)$ components. The CD band of the fluoro complex with *S*,*S*-stien in the second band region corresponds to the ^4E_b absorption component, and is of opposite sign to the ^4E_a component. The fact that the ^4E_b CD component are not observed for the fluoro complexes with *R*-pn and *S*,*S*-2,4-ptn may be responsible for the overlapping with the $^4B_2$ component which may have the same sign as the ^4E_b one. Thus, it is seen that the CD sign of the ^4E_b component for the fluoro complexes in the second band region is opposite to those for the chloro and bromo complexes. This fact may be elucidated by taking into consideration of the configuration interaction between the ^4E_a and ^4E_b states. The magnetic dipole forbidden ^4E_b←$^4B_1$ transition borrows its magnetic transition dipole moment from that for the magnetic dipole allowed ^4E_a←$^4B_1$ transition through the configuration interaction between the ^4E_a and ^4E_b states in tetragonal field, of which the off-diagonal element, $\langle ^4E_a | V(D_{4h}) | ^4E_b \rangle$, is given as $(\sqrt{3}/2)\delta\sigma$.[30] The AOM parameter, $\delta\sigma$, is defined as the splitting of one electron level of the e_g(d) orbital in tetragonal field and can be estimated from the observed splittings of the first and second octahedral bands. Thus, the rotational strength for the ^4E_b←$^4B_1$ transition is expressed as follows.

$$R(^4E_b) = (\sqrt{3}/2)\delta\sigma / \{E(^4E_b) - E(^4E_a)\} \cdot \\ \mathrm{Im}\langle ^4E_a | M | ^4B_1 \rangle \cdot \langle ^4B_1 | P | ^4E_b \rangle$$

where M and P are magnetic and electric dipole operator, respectively, and Im means the "imaginary part of". Since the energy denominator, $E(^4E_b)-E(^4E_a)=36B+\delta\sigma$, is usually positive, the sign of the $R(^4E_b)$ is governed by that of $\delta\sigma$. According to the measurements of single crystal polarized absorption spectra as well as theoretical crystal field calculations,[4] the $\delta\sigma$ value for *trans*-[CrX_2(en)$_2$]$^+$ complex has been estimated to be +600, −1240 and −1780 cm^{-1}, for the fluoro, chloro and bromo complex, respectively. The $\delta\sigma$ values for the present complexes do not seem to differ largely from those for the ethylenediamine complexes, for the ligand field strengths of these complexes are close to each other. Therefore, the sign inversion of the ^4E_b CD component from the fluoro to the chloro and bromo complexes is responsible for that of the $\delta\sigma$ parameter. A similar formulation can be also applied to the CD behaviors of the corresponding Co(III) complexes. It has been found that all the *trans*-difluoro, dichloro and dibromo(*l*-cyclohexanediamine)cobalt(III) complexes give the positive CD sign in the $^1E_b(^1T_2)$ component.[31] This finding is in accordance with the $\delta\sigma$ parameters for the three complexes having the same sign (negative).[31]

4) CD Spectra in the Spin-forbidden Transitions. a) General Considerations: The splitting of the doublet excited states in tetragonal field occurs as shown in Fig. 7. Although each the $^2E(^2T_1)$ and the ground $^4B_1(^4A_2)$ state is split into two Kramers doublets by a spin-orbit coupling, these splittings are estimated to be too small to be resolved spectroscopically at room temperature.[8b] Thus, in this case, these will be ignored and only four electronic spin-forbidden transitions, $^2A_1(^2E)$, $^2B_1(^2E)$, $^2E(^2T_1)$ and $^2A_2(^2T_1)$←$^4B_1(^4A_2)$, will be taken into account throughout the following discussion. Contrary to the expectation, however, more than four sharp but weak CD peaks are observed for the present complexes. This fact indicates the appearance of vibronic structures as discussed later.

The Rotational Strengths for the Spin-forbidden Transitions. For tetragonal chromium(III) complexes,

TABLE 2. ROTATIONAL STRENGTHS FOR THE SPIN-FORBIDDEN $^2\Gamma \leftarrow {}^4B_1$ TRANSITIONS IN TETRAGONAL CHROMIUM(III) COMPLEXES

		in unit of $\zeta'^2/18\{\Delta E(^2\Gamma)\}^2$	
^2E	$^2A_1$	$24R(^4E)$	$(1/3)(3\zeta_3'^2+\zeta_4'^2)\varepsilon_1^{-2}\cdot R(^4E)$
	$^2B_1$	$8\{R(^4E)+4R(^4B_2)\}$	$(1/9)(3\zeta_3'^2+\zeta_4'^2)\varepsilon_1^{-2}\cdot R(^4E)+(16/9)\zeta_1'^2\varepsilon_2^{-2}\cdot R(^4B_2)$
$^2T_1$	^2E	$6\{R(^4E)+2R(^4B_2)\}$	$(1/12)(3\zeta_2'^2+\zeta_1'^2)\varepsilon_1^{-2}\cdot R(^4E)+(2/3)\zeta_4'^2\varepsilon_2^{-2}\cdot R(^4B_2)$
	$^2A_2$	$6R(^4E)$	$(1/12)(3\zeta_3'^2+\zeta_4'^2)\varepsilon_1^{-2}\cdot R(^4E)$

$\Delta E(^2\Gamma) = E(^2\Gamma)-E(^4\Gamma)$; ζ_1', ζ_2', ζ_3' and ζ_4' are the effective spin-orbit coupling constants as defined in the text. ε_1 and ε_2 are the energy interval between the $^2\Gamma$ and ^4E and between the $^2\Gamma$ and $^4B_2$, respectively.

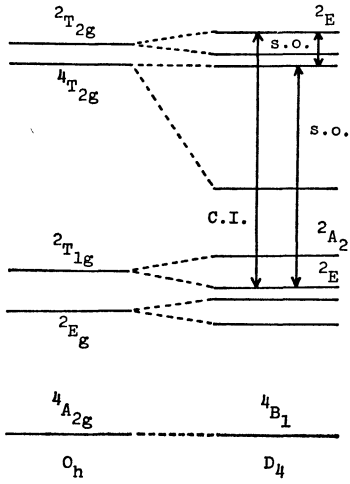

Fig. 7. Energy levels of a tetragonal chromium(III) ion. The vertical lines indicate the configuration interaction (C. I.) among the ^2E states or the spin-orbit coupling (s. o.) between the ^2E and the quartet state.

the spin-forbidden $^2\Gamma(t_2^3)\leftarrow{}^4B_1(t_2^3)$ transitions attain their rotational strengths by aquiring a small part, $(k\zeta'/\Delta E)^2$, of the rotational strengths for the nearby spin-allowed and magnetic dipole allowed $^4E(t_2^2e)$, $^4B_2(t_2^2e)\leftarrow{}^4B_1(t_2^3)$ transitions, as given by

$$R(^2\Gamma) = (k\zeta'/\Delta E)^2R(^4\Gamma) \qquad (1)$$

where k is a numerical coefficient, and ζ' is a spin-orbit coupling constant, $\zeta'=(\sqrt{2}/6)i\langle t_2|H_{SO}|e\rangle$, and ΔE refers to the energy interval between the $^2\Gamma$ and $^4\Gamma$, and $R(^4\Gamma)$ is the rotational strengths for the tetragonal splitting components of the $^4T_2$, $R(^4E)=2\mathrm{Im}\langle^4E|P|^4B_1\rangle\cdot\langle^4B_1|M|^4E\rangle$ and $R(^4B_2)=\mathrm{Im}\langle^4B_2|P|^4B_1\rangle\cdot\langle^4B_1|M|^4B_2\rangle$. The $k^2R(^4\Gamma)$ in the Eq. (1) are obtained by using the Wigner and Clebsh-Gordan coefficients with tetragonal field in the absence of vibronic contribution[32,33] as in the case of trigonal complexes[1] as shown in the third column of Table 2. This approximation seems to be valid, since it is inferred that CD intensity is static in origin for the corresponding tetragonal Co(III) complexes.[29] This Table shows that the $^2A_2\leftarrow{}^4B_1$ and $^2A_1\leftarrow{}^4B_1$ transitions borrow their rotational strengths only from the $R(^4E)$ and hence they should have the same sign. In the cases of the $R(^2B_1)$ and $R(^2E)$ to which both the $R(^4E)$ and $R(^4B_2)$ contribute, however, more exact examinations of $\zeta'/\Delta E$ are required. As seen in section *1)*, the energy separation between the $^4B_2$ and ^4E states is so large that the difference between $\varepsilon_1=E(^2\Gamma)-E(^4E)$ and $\varepsilon_2=E(^2\Gamma)-E(^4B_2)$ needs to be taken into consideration. For the complexes concerned, ε_1 depends on axial ligands, increasing in the order of the fluoro, chloro and bromo complexes and ε_2 is almost constant. Assuming no spin-orbit effect on ligands, the terms involving the $R(^4E)$ give larger contribution to the $R(^2\Gamma)$ by a factor of $(\varepsilon_2/\varepsilon_1)^2$ than those involving the $R(^4B_2)$, for the $(\varepsilon_2/\varepsilon_1)^2$ is found to be ~3 for the fluoro, ~4—~5 for the chloro and ~7—~8 for the bromo complexes. In addition, the ratio between the contribution of the $R(^4E)$ to that of the $R(^4B_2)$ is governed by the kinds of optically active diamines. That is, it is found that the $|R(^4E)/R(^4B_2)|$ obtained from the observed CD spectra is about 3 to 6 for the *R*-pn complexes and about 1 for the *S*,*S*-stien and *S*,*S*-2,4-ptn complexes. Consequently, it is expected that the $R(^2\Gamma)$ increase in the order of the fluoro, chloro and bromo complexes and that the contribution from the terms involving the $R(^4E)$ is large in comparison with those involving the $R(^4B_2)$. These are contrary to the findings. That is, the CD intensities in the spin-forbidden transitions decrease in the order of the fluoro, chloro and bromo complexes and they do not always exhibit the same sign as that of the ^4E component, as in Figs. 8—10 and Table 1. These facts suggest the importance of a spin-orbit effect on the ligands.

According to a simple molecular orbital treatment, it has been shown that the spin-orbit effects on the halogeno ligands in $[CoX(NH_3)_5]^{2+}$ play an important role in gaining the spin-forbidden absorption band intensities.[34,35] The application of this MO treatment to the tetragonal Cr(III) complexes leads to four nonequivalent effective spin-orbit coupling constants. Assuming no π bonding between the metal and amine ligands, one electron antibonding LCAO-MO for the *trans*-$[CrX_2(N)_4]$ type complexes is given as follows.[4]

$$\left.\begin{aligned}
a_1(e) &= N_{\sigma X}[a_1(d_{z^2})-\lambda_{\sigma X}\textstyle\sum p_{zi}(X)]\\
b_1(e) &= N_{\sigma N}[b_1(d_{x^2-y^2})-\lambda_{\sigma N}\textstyle\sum p_{zi}(N)]\\
a_2(t_2) &= a_2(d_{xy})\\
e(t_2) &= N_{\pi X}[e(d_{xz})-\lambda_{\pi X}\textstyle\sum\{p_{xi}(X)-p_{xj}(X)\}]\\
e(t_2) &= N_{\pi X}[e(d_{yz})-\lambda_{\pi X}\textstyle\sum\{p_{yi}(X)-p_{yj}(X)\}]
\end{aligned}\right\} \qquad (2)$$

where $N_{\sigma N}$, $N_{\sigma X}$, $N_{\pi X}$ and $\lambda_{\sigma N}$, $\lambda_{\sigma X}$, $\lambda_{\pi X}$ are normalizing and admixture coefficients, respectively, $\sum p(N)$ and $\sum p(X)$ stand for symmetry adapted linear combinations of p orbitals of nitrogens and halogens, respectively, and $a_1(d_{z^2})$ *etc.* are pure d orbitals. The

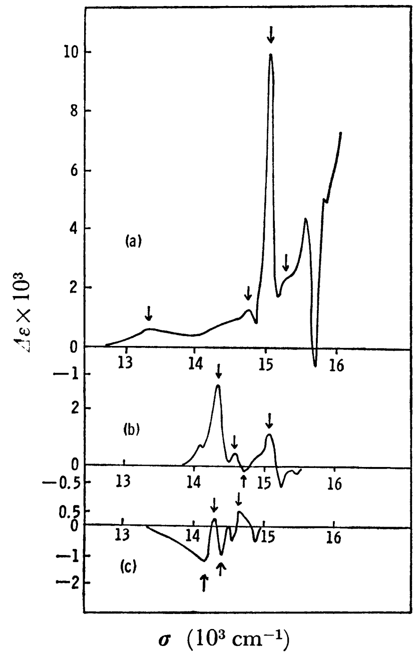

Fig. 8. CD curves in the spin-forbidden transitions of *trans*-$[CrX_2(R\text{-pn})_2]^+$ (a) X=F, (b) X=Cl, (c) X=Br. The arrows indicate the electronic states assigned in the text.

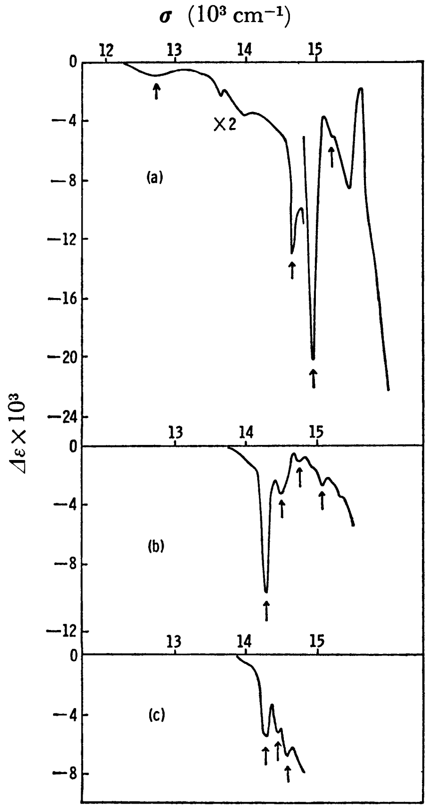

Fig. 9. CD curves in the spin-forbidden transitions of *trans*-$[CrX_2(S,S\text{-stien})_2]^+$ (a) X=F, (b) X=Cl, (c) X=Br. The arrows as in Fig. 8.

upper two e orbitals and lower two t_2 orbitals are σ- and π-antibonding MO's, respectively. By using these molecular orbitals, the molecular orbital matrix elements, $\langle t_2|H_{so}|e\rangle$, are evaluated as,[33]

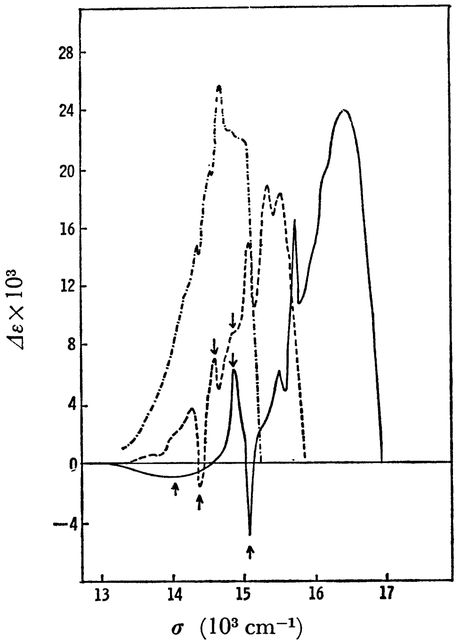

Fig. 10. CD curves in the spin-forbidden transitions of *trans*-$[CrX_2(S,S\text{-}2,4\text{-ptn})_2]^+$, X=F (——) in water; X=Cl (----) in methanol; X=Br (—·—·—) in methanol. The arrows as in Fig. 8.

$$\left.\begin{aligned}\zeta_1' &= (\sqrt{2}/6)i\langle a_2(t_2)|H_{so}|b_1(e)\rangle = N_{\sigma N}\zeta_d' \\ \zeta_2' &= (\sqrt{2}/6)i\langle a_2(t_2)|H_{so}|a_1(e)\rangle = N_{\sigma X}\zeta_d' \\ \zeta_3' &= (\sqrt{2}/6)i\langle e(t_2)|H_{so}|a_1(e)\rangle \\ &= N_{\pi X}N_{\sigma X}\{\zeta_d' - (1/2)\lambda_{\pi X}\lambda_{\sigma X}\zeta_p\} \\ \zeta_4' &= (\sqrt{2}/6)i\langle e(t_2)|H_{so}|b_1(e)\rangle \\ &= N_{\pi X}N_{\sigma N}\zeta_d'\end{aligned}\right\} \qquad (3)$$

where ζ_d' and ζ_p are the spin-orbit coupling constants of pure 3d orbitals of Cr(III) ion and of p orbitals of halogen, respectively. It is noted that the ζ_1' and ζ_3' correspond to the effective spin orbit coupling constant for $Cr(N)_6^{3+}$ and $Cr(X)_6^{3-}$, respectively. Since the ζ_3' is given as a linear combination of ζ_d' and ζ_p, the value of ζ_3' varies with the halogen ligands. The Eq. (3) may be rewritten in terms of the relativistic nephelauxetic ratios, $\beta^*(N)$ for the amine ligand and $\beta^*(X)$ for the halogen ligands as follows. $\zeta_1'=\beta^*_{35}(N)\text{-}\zeta_d'$, $\zeta_2'=\sqrt{\beta^*_{33}(X)\ \beta^*_{55}(N)}\ \zeta_d'$, $\zeta_3'=\beta^*_{35}(X)\ \zeta_d'$, $\zeta_4'=\sqrt{\beta^*_{33}(N)\ \beta^*_{55}(X)}\ \zeta_d'$, where ζ_p in ζ_3' is ignored. The $\beta^*_{55}(N)$ is mainly due to the relativistic nephelauxetic effect caused by the central field covalency.[36] Using these correlations, the ζ_2' and ζ_4' are connected with the ζ_3' and ζ_1' through the $\beta^*_{55}(N)$ and $\beta^*_{55}(X)$, as shown in the following. $\zeta_4'=\sqrt{\beta^*_{55}(X)/\beta^*_{55}(N)}\ \zeta_1'$; $\zeta_2'=\sqrt{\beta^*_{55}(N)/\beta^*_{55}(X)}\ \zeta_3'$, hence $\zeta_4'/\zeta_3'=\zeta_1'/\zeta_2'$, where it is assumed that $\beta^*_{35}=\sqrt{\beta^*_{33}\,\beta^*_{55}}$.[36] In this case, the values of the four constants seem close each other. In the case of the complexes having heavy ligands with large ζ_p, however, the substantial decrease in ζ_3' may be expected owing to the subtractive contribution of the terms involving the ζ_p to the ζ_3', assuming appropriate values of the ligand admixture coefficient, $\lambda_{\pi X}\lambda_{\sigma X}$.[37] Therefore, the difference between the ligand-dependent spin-orbit coupling constant ζ_3' and the other constants must be taken into consideration.

By introducing four different effective spin-orbit coupling constants in terms of the strong field wave functions of d^3 configurations in tetragonal field,[2] together with two kinds of the energy denominator, ε_1^{-1} and ε_2^{-1}, the refined rotational strengths for the spin-forbidden transitions can be represented as in the fourth column of Table 2. It is seen that most of the $R(^2\Gamma)$'s are rather sensitive to the ζ_3' and decrease with increasing ζ_p in the order of the fluoro, chloro and bromo complexes. This order is consistent with the observation.* As for the sign of the CD components, in either case of the complexes with vanishingly small ζ_3', or the complexes having $(\varepsilon_2/\varepsilon_1)^2<4$ and almost equal effective spin-orbit coupling constants, only the $R(^2B_1)$ among the four $R(^2\Gamma)$'s may be expected to exhibit the same sign as the $R(^4B_2)$, and the rotational strengths for the remaining spin-forbidden transitions are predicted to be of the same sign as the $R(^4E)$ for any axial ligands. It appears that this prediction holds for the *S,S*-stien complexes, though these complexes show two same signed CD bands in the first spin-allowed transition region. For the complexes with oppositely signed CD bands in the first spin-allowed transitions, some oppositely signed CD components are observed also in the spin-forbidden transitions as shown in Figs. 8 and 10. Such a CD behavior, however, was not elucidated by the spin-orbit coupling mechanism, only between the ^2E, $^2T_1$ and the $^4E(^4T_2)$, $^4B_2(^4T_2)$ states. Thus some additional contributions from the terms involvong the $R(^4B_2)$ become needed in terms of another mechanism.

More exact consideration including the configuration interaction accounts for the large mixing of the $^4B_2$ state into the doublet states. Of the doublet states, the $^2E(^2T_2)$ is strongly mixed with the $^4B_2$ state through a spin-orbit coupling, because these states lie very closely in the crystal field approximation. This strong coupling is substantiated from the fact that the $^4B_2$ component is split into double peaks in the absorption and CD spectra as in Figs. 1—2 and 4—6. In addition, the configuration interaction between the $^2E(^2T_2)$ and $^2E(^2T_1)$ occurs in tetragonal field. The off-diagonal matrix element is obtained as $3Ds-5Dt=2\delta\pi$, where Ds, Dt and $\delta\pi$ are the crystal field and AOM parameter, respectively.[2] The consequence of this configuration interaction has been discussed in photochemical implication for chromium(III) complexes[39] and in relation to the lower frequency shift of the $^2E(^2T_1)$ state.[14] The spin-orbit coupling gives rise to large admixture of the $^4B_2$ into the $^2E(^2T_2)$, and the $^4B_2$ mixes with the $^2E(^2T_1)$ through the configuration interaction with the $^2E(^2T_2)$ as in Fig. 7. The operation of these interactions gives additional rotational strengths for the $^2E(^2T_1)\leftarrow{}^4B_1(^4A_2)$ spin-forbidden transition by $(2/3)\varepsilon_4^{-2}\cdot\varepsilon_3^{-2}\cdot\zeta_4'^2\cdot 4(\delta\pi)^2\cdot R(^4B_2)$, where ε_4 and ε_3 are the energy interval between the $^2E(^2T_2)$ and $^4B_2$ $(=10Dq-15B-5C)$ and between the $^2E(^2T_1)$ and $^2E(^2T_2)$ $(=6B+2C)$, respectively. Then the contribution of the terms involving the $R(^4B_2)$ to the $R(^2E(^2T_1))$ becomes $(2/3)\zeta_4'^2\varepsilon_2^{-2}\{1+4\varepsilon_4^{-2}(\delta\pi)^2\}\cdot R(^4B_2)$, assuming $\varepsilon_3\simeq\varepsilon_2$. The value of $\delta\pi$ is found to be of the order of 1000 cm^{-1} from the crystal field approximations and single crystal polarized absorption spectra of *trans*-$[CrX_2(en)_2]^+$. The ε_4 seems to be of the order of 1000 cm^{-1} or less. In the strong coupling case of $E(^4B_2)\simeq E(^2E(^2T_2))$ with zero spin-orbit coupling, the ε_4 is equal to $(\sqrt{3}/2)\zeta_4'$ and thus being estimated to be 100—200 cm^{-1}. Then the additional rotational strengths are sensitive to the ε_4 and in some cases, are expected to be so large that the term involving the $R(^4B_2)$ overwhelms that involving the $R(^4E)$.**

From these considerations, it may be summarized that the $R(^2A_1)$ should be the most intense and four times as large as the $R(^2A_2)$, and they should have the same sign as the $R(^4E)$. Further, the $R(^2E)$ and $R(^2B_1)$ are not always of the same sign as the $R(^4E)$.

b) The Assignments of the CD Components. The Fluoro Complexes with R-*pn and* S,S-*stien.* The crystal field theory predicts the positions and the splittings of the doublet states. In general, the ^2E cubic parent component lies at the lower frequency by about 700 cm^{-1} than the $^2T_1$ one. According to Macfarlane's approximation,[10a] the splitting of the ^2E cubic state into $^2A_1$ and $^2B_1$ in tetragonal field may be calculated in terms of the parameters, $\delta\sigma$, $\delta\pi$, $10Dq$, B and C; *i.e.*,

$$E(^2A_1)-E(^2B_1)=192B^2/(10Dq+14B+3C)\times\{\delta\pi/(10Dq+14B+3C)+\delta\sigma/(10Dq+5B)\}\tag{4}$$

On the other hand, owing to the configuration interaction between the $^2E(^2T_1)$ and $^2E(^2T_2)$ states, the $^2E(^2T_1)$ state is shifted by $4(\delta\pi)^2/\varepsilon_3$ to the lower frequency side. The former Eq. (4) leads to the expectation that the $^2B_1$ state for the fluoro complexes always locates at the lower frequency side than the $^2A_1$ because of positive sign of both the $\delta\pi$ and $\delta\sigma$.[3–6] The shift of the $^2E(^2T_1)$ state is sensitive to the value

---

* In the case of Co(III) complexes, the molecular spin-orbit coupling constants corresponding to the ζ_3', $\zeta=(-i/3)\langle t_2|H_{so}|t_2\rangle$, are given as an additive contribution of the terms involving ζ_p of halogeno ligands.[33] Thus, this constants increase with increasing ζ_p and in the order of the fluoro, chloro and bromo complexes. This order agrees with that obtained from the spin-forbidden absorption intensities.[38] On the other hand, for the Cr(III) complexes, the intensity order of the spin-forbidden absorption bands is contrary to that of CD intensities in the spin-forbidden transitions. This finding can not be interpreted in the course of the present discussion, since the sharp spin-forbidden bands are overlapped with the lower frequency envelope of the broad first spin-allowed bands to increasing extent in the order of the fluoro, chloro and bromo complexes.

** In the case of $[Cr(en)_3]^{3+}$, the similar configuration interaction between the $^2E(^2T_1)$ and $^2E(^2T_2)$ state and/or $^2E(^2E)$ and $^2E(^2T_2)$ state and the strong spin-orbit coupling between the $^2E(^2T_2)$ and $^4E(^4T_2)$ or $^4A_1(^4T_2)$ state can occur. The off-diagonal elements of these configuration interactions are proportional to the trigonal splitting parameter K. [S. Sugano and M. Peter, *Phys. Rev.*, **122**, 381 (1961).] In this case, however, the mixing of the $^2E(^2T_2)$ state with the $^2E(^2E)$ and $^2E(^2T_1)$ state seems to be negligible owing to small K value. [A. J. McCaffery, S. F. Mason, and B. J. Ballard, *J. Chem. Soc.*, **1965**, 5094.] In the trigonal case, therefore, these interactions may be ignored.

of $\delta\pi$, because ε_3 includes only the Racah electronic repulsion parameters, and hence almost independent on the ligand field. Thus, the $^2E(^2T_1)$ state for the fluoro complexes seems to be shifted to the lower frequency than that for the other aniono complexes, because the $\delta\pi$ value of the fluoro complexes is largest in the three halogeno complexes.[4] Then the $^2A_2(^2T_1)$ state locates at the highest frequency. In fact, from the luminescence and absorption spectra of *trans*-[CrF$_2$(en)$_2$]ClO$_4$ and its iodide, Flint *et al.*[14] have revealed that the lowest frequency phosphorescence band at 13098 cm^{-1} is assigned to the $^2E(^2T_1)$ state and the $^2B_1$, $^2A_1$ and $^2A_2$ states locate at 14860, 15052 and 15270 cm^{-1}, respectively, in spite of a number of observed vibronic structures. This assignment is also consistent with the prediction based on the crystal field theory. By collating this assignment with the CD components of the present fluoro complexes, the peaks are assigned on the assumption that the crystal field parameter values of the optically active diamine complexes are close to those of the ethylenediamine complex. For the *R*-pn complex, the lowest frequency positive CD peak at 13330 cm^{-1} is due to the $^2E(^2T_1)$ state, and the weak positive peak at 14730 cm^{-1} and the strongest positive peak at 15030 cm^{-1} are due to the $^2B_1$ and $^2A_1$ state, respectively, as in Fig. 8 a). The $^2A_2$ state may correspond to the shoulder near 15300 cm^{-1} of positive sign. The theoretical correlation between the rotational strengths in the spin-forbidden transitions and those in the spin-allowed transitions can account for the CD behaviors of these peaks semi-quantitatively. That is, the $^2A_1$ peak is the strongest and about four times as strong as the $^2A_2$ one as mentioned before. The weak intensities of the ^2E and $^2B_1$ peaks may be responsible for the increasing contribution of the terms involving the $R(^4B_2)$. That the ^2E peak of the fluoro complex is of the same sign as the ^4E one suggests a weak spin-orbit coupling between the $^2E(^2T_2)$ and $^4B_2$ state. In fact, no double peaks of the $^4B_2$ component is observed in absorption and CD spectra of the fluoro *R*-pn complex. Although a negative peak is observed at 15680 cm^{-1}, no negative sign is expected in this region. The vibronic CD theory for electric dipole forbidden and magnetic dipole allowed transitions which are spin-allowed either in zeroth order or in first order *via* a spin-orbit coupling expects the mixed signs of CD and that vibrational progressions of totally symmetric modes on electronic origins should contribute to CD spectra.[40] Therefore, this CD peak with negative sign together with other positive peaks unassigned may be due to the vibronic bands.*** The strong intensities of vibronic bands observed in CD are compatible with those in absorption spectra.[14]

For the *S*,*S*-stien complex (Fig. 9 a), the 12700 cm^{-1} peak with negative sign may be assigned to the $^2E(^2T_1)$ state. It appears that the $^2B_1$ and $^2A_1$ state correspond to a weak 14650 cm^{-1} and a strong 14950 cm^{-1} peak, respectively. The 15210 cm^{-1} peak is due to the $^2A_2(^2T_1)$ state, of which the CD intensity is about one fourth of that of the $^2A_1$ peak. The remaining peaks may be ascribed to the vibronic origins. It seems plausible that the CD signs of these peaks agree with those of the CD bands in the first spin-allowed transitions.

The Chloro Complexes with R-*pn and* S,S-*stien.* The luminescence spectrum of *trans*-[CrCl$_2$(en)$_2$]$^+$ has shown that the lowest frequency doublet state locates at 14380 cm^{-1}.[11] For the *S*,*S*-stien complex, the lowest frequency negative CD peak at 14270 cm^{-1} is the most intense and hence this peak is assigned to the $^2A_1$ state. The next-neighbouring peak at 14500 cm^{-1} may be due to the $^2B_1$ state. The CD peak at 15070 cm^{-1} may be assigned to the $^2A_2$ state, because the CD intensity of this peak is about one fourth of that of the $^2A_1$ component, as theoretically expected. Further, since the ^2E state is expected to lie at the lower frequency than the $^2A_2$ state, the CD peak at 14810 cm^{-1} may be assigned to the ^2E state.

The most intense CD peak of the *R*-pn complex at 14340 cm^{-1} may be due to the $^2A_1$, and it seems that the $^2B_1$, ^2E and $^2A_2$ state correspond to the 14580, 14700 and 15020 cm^{-1} peaks, respectively, although the lowest frequency peak at 14080 cm^{-1} can not be identified. In this complex also the $^2A_2$ peak is weaker than the $^2A_1$ one. It needs to be noted that the $^2E(^2T_1)$ component is negative and of the same sign as the $^4B_2$ one. This sign inversion may be attributed to that a spin-orbit coupling between the $^2E(^2T_2)$ and $^4B_2$ state is strong enough to cause the additional contribution of the term involving the $R(^4B_2)$, $(2/3)\zeta_4'^2\varepsilon_2^{-2}\{1+4\varepsilon_4^{-2}(\delta\pi)^2\}\cdot R(^4B_2)$, and to overcome the term involving the $R(^4E)$, $(1/12)(3\zeta_2'^2+\zeta_1'^2)\varepsilon_1^{-2}\cdot R(^4E)$, as discussed in the previous section. In fact, such a strong spin-orbit coupling gives rise to the splitting of the $^4B_2$ component in absorption spectra by about 400 cm^{-1} as in Fig. 1. The positions and the splitting of the doublet states of this complex is in accordance with the crystal field calculation for the corresponding ethylenediamine complex.[2,3] The remaining CD peaks may be due to the vibronic bands, though some negative peaks are observed.

The Bromo Complexes with R-*pn and* S,S-*stien.* The *R*-pn complex gives only two positive CD peaks at 14290 cm^{-1} and 14650 cm^{-1} (Fig. 8c). Thus, the lower frequency 14290 cm^{-1} peak and the higher frequency 14650 cm^{-1} peak are assigned to the $^2A_1$ and $^2A_2$ state, respectively, because their rotational strengths should have the same sign as the $R(^4E)$ and the $^2A_1$ state should lie at the lower frequency than the $^2A_2$ state from a theoretical point of view. Contrary to the other complexes mentioned before, however, the $^2A_2$ peak is more intense than the $^2A_1$ one. This may be due to the large mutual cancellation among the neighbouring CD peaks with alternate signs. For the bromo complexes, the crystal field approximation predicts the lowest frequency shift of the $^2E(^2T_1)$ state.[2,3] Therefore, a negative CD peak at 14080 cm^{-1} may be due to the ^2E state. The negative sign of this

---

*** The influences of the methyl group of *R*-pn in the present complex on the vibronic CD bands are disregarded, since the CD pattern in the spin-forbidden transitions of the fluoro complex with *R*-pn is found to be quite identical with that of the fluoro complex with *R*,*R*-cyclohexanediamine which was prepared by the method of Glerup *et al.*[22]

peak implies a strong spin-orbit coupling between the $^2E(^2T_2)$ and $^4B_2$ state, which may give rise to the splitting of the $^4B_2$ component in CD spectrum of this complex as in Fig. 4. The $^2B_1$ state may correspond to a negative peak at 14390 cm^{-1}. The negative sign of the $^2B_1$ state is caused by the vanishing decrease in ζ_3' owing to the large ζ_p of the axial ligand, in which case the term involving the $R(^4B_2)$ is $16(\zeta_1'/\zeta_4')^2(\varepsilon_1/\varepsilon_2)^2$ times as large as that involving the $R(^4E)$ and, assuming $(\varepsilon_1/\varepsilon_2)^2 \simeq 1/8$ and $(\zeta_1'/\zeta_4')^2 = \beta^*_{55}(N)/\beta^*_{55}(Br) \gg 1$, thus overwhelming the $R(^4E)$.

From comparison with the *R*-pn complex, three CD peaks observed for the *S,S*-stien complex are assigned to the $^2A_1$, $^2B_1$ and $^2A_2$ state from the lower frequency side, respectively, though the ^2E component is missing.

The S,S-*2,4-ptn Complexes.* The *S,S*-2,4-ptn complexes show anomalous CD patterns in the spin-forbidden band region, compared with the *R*-pn and *S,S*-stien complexes as in Fig. 10. That is, relatively intense structural CD bands with positive sign are observed in the region of 16500−14500 cm^{-1}. Although the shift pattern with varying the axial ligands is similar to that of the ^4E component, suggesting that these bands seem to be associated with the spin-allowed transitions, they can not be assigned at the present. The spin-forbidden transitions may occur at the lower frequency side than these anomalous CD bands, but overlapping of some of them with the anomalous bands makes their assignments difficult. The tentative assignments are made as follows. For the fluoro complex, the lowest frequency CD peak at 13950 cm^{-1} with negative sign may be due to the ^2E state, and the 14850 cm^{-1} and 15080 cm^{-1} peaks to the $^2B_1$ and $^2A_1$ states, respectively, as in the case of the other fluoro complexes. It seems plausible that the $^2A_1$ peak exhibits the same sign as the ^4E one. The $^2B_1$ peak is of the same sign as the $^4B_2$ one. This is because of the $(\varepsilon_2/\varepsilon_1)^2 \simeq 3$ and $R(^4E)/R(^4B_2) \simeq -1$ and hence $R(^2B_1) = (4/9)\zeta_1'^2\varepsilon_1^{-2}\{R(^4E) + 4/3R(^4B_2)\} \simeq (4/27)\zeta_1'^2\varepsilon_1^{-2}R(^4B_2)$ where $\zeta_1' \simeq \zeta_2' \simeq \zeta_3' \simeq \zeta_4'$ for the fluoro complex with *S,S*-2,4-ptn. The $^2A_2$ peak is obscured by the rather intense positive band. For the chloro complex, only one negative CD peak was observed at 14410 cm^{-1} and this may be due to the $^2A_1$ state. The 14590 cm^{-1} peak with positive sign may be assigned to the $^2B_1$ state, since the crystal field calculation predicts that the $^2B_1$ state lies at the higher frequency side of the $^2A_1$ state. The positive sign of the $^2B_1$ state may be caused by the considerable decrease in ζ_3' owing to the large ζ_p and the increasing contribution of the term involving the $R(^4B_2)$, as in the case of the bromo complex with *R*-pn. The $^2E(^2T_1)$ state may correspond to a positive peak observed at 14880 cm^{-1}. This positive sign may be attributed to a strong spin-orbit coupling as found for the chloro complex with *R*-pn. For the bromo complex, only in view of the transition energies, the 14330, 14510, and 14640 cm^{-1} CD peaks may be due to the $^2A_1$, $^2B_1$ and $^2A_2$ state, respectively, although their signs are all positive.

Conclusion. On the basis of the assignments thus obtained for the three series of complexes as in Table 1, it has been found that the positions of the $^2A_1$ state are shifted to the lower frequency in the order of the fluoro, chloro and bromo complexes, demonstrating the nephelauxetic effect.37) The splitting of the ^2E cubic state, $E(^2A_1) - E(^2B_1)$, is found to be about +300 cm^{-1} for the fluoro, about −250 cm^{-1} for the chloro and −100 to −150 cm^{-1} for the bromo complexes, although the *S,S*-2,4-ptn complexes give somewhat smaller splittings. The splitting obtained for the chloro and bromo complexes is in an order of magnitude larger than the theoretical value estimated from Macfarlane's approximation on the crystal field calculation. That is, the theoretical splittings are obtained as +180, −41 and −11 cm^{-1} for the fluoro, chloro and bromo complexes, respectively, by using the parameter values estimated by Dubicki *et al.*4) As observed12,13) and discussed for the pentaammine aniono Cr(III) complexes by Flint and Matthews,13) such a large splitting of the ^2E cubic state can not be elucidated by the crystal field theory. The positions of the $^2E(^2T_1)$ state vary with the coordinated diamines, *i.e.*, 13098 cm^{-1} for the en complex,14) 13330 cm^{-1} for the *R*-pn complex, 12710 cm^{-1} for the *S,S*-stien complex, and 13950 cm^{-1} for the *S,S*-2,4-ptn complex. This is probably caused by variation of the parameters $\delta\pi$ and ε_3 for the diamines.

References

1) S. Kaizaki, J. Hidaka, and Y. Shimura, *Inorg. Chem.*, **12**, 142 (1973).

2) J. R. Perumareddi, *Coord. Chem. Rev.*, **4**, 73 (1969); J. R. Perumareddi, *J. Phys. Chem.*, **71**, 3155 (1967).

3) L. Dubicki and R. L. Martin, *Austral. J. Chem.*, **22**, 839 (1969).

4) L. Dubicki, M. A. Hitchman, and P. Day, *Inorg. Chem.*, **9**, 188 (1969); L. Dubicki and P. Day, *ibid.*, **10**, 2043 (1971).

5) R. L. Klein, Jr., N. C. Miller, and J. R. Perumareddi, *Inorg. Chim. Acta*, **7**, 685 (1973).

6) J. Glerup and C. E. Schäffer, Prog. Coord. Chem., Proceed. 11th ICCC (1968), p. 500.

7) W. W. Fee and J. N. MacB. Harrowfield, *Austral. J. Chem.*, **23**, 1049 (1969).

8) H. Yamatera, This Bulletin, **31**, 95 (1958); D. S. McClure, "Advances in the Chemistry of the Coordination Compounds," S. Kirschner, Ed., Macmillan, New York, N.Y., (1961), p. 498; C. E. Schäffer and C. K. Jørgensen, *Kgl. Danske Videnskab. Mat. -fys. Medd.*, **34**, No. 13 (1965).

9) J. C. Donini, B. R. Hollebone, G. London, A. B. P. Lever, and J. C. Hempel, *Inorg. Chem.*, **14**, 455 (1975); T. J. Barton and R. C. Slade, *J. Chem. Soc., Dalton*, **1975**, 650.

10) a) R. M. Macfarlane, *J. Chem. Phys.*, **47**, 2066 (1967); b) W. M. Fairbank, Jr. and G. K. Klauminzer, *Phys. Rev., B*, **7**, 500 (1973).

11) G. B. Porter and H. L. Schläfer, *Z. Phys. Chem.*, **40**, 280 (1964).

12) W. N. Shepard and L. S. Forster, *Theoret. Chim. Acta*, **20**, 135 (1971).

13) C. D. Flint and A. P. Matthews, *J. Chem. Soc., Faraday Trans. II*, **69**, 419 (1973).

14) C. D. Flint and A. P. Matthews, *ibid.*, **70**, 1307 (1974).

15) R. K. Rowry, Jr. and J. R. Perumaredii, *J. Phys. Chem.*, **74**, 1371 (1970).

16) C. J. Hawkins, E. Larsen, and I. Olsen, *Acta Chem. Scand.*, **19**, 1915 (1965).

17) S. F. Mason, *J. Chem. Soc. A*, **1971**, 667.

18) F. Mizukami, H. Ito, J. Fujita, and K. Saito, This Bulletin, **45**, 2129 (1972).

19) B. Bosnich and J. MacB. Harrowfield, *J. Amer. Chem. Soc.*, **94**, 3425 (1972).

20) O. F. Williams and J. C. Bailar, Jr., *ibid.*, **81**, 4464 (1959).

21) I. Lifschitz and J. G. Bos, *Rec. Trav. Chim.*, **59**, 173 (1940).

22) J. Glerup, J. Josephsen, K. Michelsen, E. Pedersen, and C. E. Schäffer, *Acta Chem. Scand.*, **24**, 247 (1970).

23) W. W. Fee, J. N. MacB. Harrowfield, and W. G. Jackson, *J. Chem. Soc.*, *A*, **1970**, 2612.

24) Y. Shimura and R. Tsuchida, This Bulletin, **29**, 311 (1956).

25) C. K. Jørgensen, "Modern Aspects of Ligand Field Theory", North-Holland Publishing Company, Amsterdam, (1971), p. 339; S. Yamada and R. Tsuchida, This Bulletin, **26**, 15 (1953).

26) a. P. L. Fereday and S. F. Mason, *Chem. Commun.*, **1971**, 1314; b. S. F. Mason and R. H. Seal, *ibid.*, **1973**, 422. The absolute configuration of $(-)_{589}$-stilbenediamine used here is consistent with that determined by Mason *et al.* in 1973; *i.e.*, the $(-)_{589}$-isomer takes (*S*,*S*)-configuration.

27) Y. Saito and H. Iwasaki, This Bulletin, **35**, 1131 (1962).

28) F. S. Richardson, *J. Chem. Phys.*, **54**, 2453 (1971).

29) R. Dingle, *ibid.*, **46**, 1 (1967).

30) R. A. D. Wentworth and T. S. Piper, *Inorg. Chem.*, **4**, 202 (1965).

31) R. S. Treptow, *ibid.*, **5**, 1593 (1966).

32) S. Sugano and Y. Tanabe, *J. Phys. Soc.*, *Japan*, **13**, 880 (1958); S. Sugano, A. L. Schawlow, and F. Varsanyi, *Phys. Rev.*, **120**, 2045 (1960).

33) S. Sugano, Y. Tanabe, and H. Kamimura, "Multiplets in Transition Metal Ions in Crystals", Academic Press, New York, N. Y. (1970), p. 273.

34) C. K. Jørgensen, *Structure and Bonding*, **1**, 3 (1966).

35) C. J. Ballhausen, *Mol. Phys.*, **5**, 461 (1963).

36) C. K. Jørgensen, "Absorption Spectra and Chemical Bonding in Complexes", Pergamon Press, Oxford, (1962), p. 134; "Oxidation Number and Oxidation State," Springer-Verlag, Berlin (1969), p. 72.

37) From the electron spin resonance studies for tetragonal Cr(III) complexes [E. Pedersen and S. Kallesoe, *Inorg. Chem.*, **13**, 1603 (1974); E. Pedersen and S. Kallesoe, *ibid.*, **14**, 85 (1975).], Pedersen *et al.* have required such a spin-orbit effect on ligands in terms of a simple molecular orbital treatment in order to elucidate the large zero field splittings of bromo and iodo complexes. Although the ESR results are apparently contrary to the present CD results, the manifold origins of the zero field splittings may be taken into consideration. [L. E. Mohrmann and B. B. Garrett, *ibid.*, **13**, 357 (1974).]

38) M. Linhard and M. Weigel, *Z. Phys. Chem*, *N. F.*, **11**, 308 (1957); J. Fujita and Y. Shimura, This Bulletin, **36**, 1281 (1963); T. Yasui and Y. Shimura, *ibid.*, **36**, 1286 (1963).

39) J. I. Zink, *Inorg. Chem.*, **12**, 1957 (1973).

40) W. Moffitt and A. Moscowitz, *J. Chem. Phys.*, **30**, 648 (1959); O. E. Weigang, Jr., *ibid.*, **43**, 3609 (1965); S. E. Harnung, E. C. Ong, and O. E. Weigang, Jr., *ibid.*, **55**, 5711 (1971); M. J. Harding, *J. Chem. Soc.*, *Faraday Trans. II*, **68**, 234 (1972).